Three-Dimensional Limit Equilibrium Stability Analysis of the Irregularly Shaped Excavation Corner with Skew Soil Nailing System

Kim, Hong-Taek[*1] Cho, Yong-Kwon[*2]
Park, Jun-Yong[*3] Lee, Hyung-Kyu[*4]

요 지

사면보강 또는 굴착면의 안정성 확보를 위해 쏘일네일링 공법이 종종 적용되고 있다. 그러나 오목형태 또는 볼록형태 모서리부와 같은 특수한 지역에 쏘일네일링 공법이 적용되어질 경우, 편기각 보강형태, 즉 skew 쏘일네일 형태로 주로 시공되고 있다.

하지만, 지금까지 skew 쏘일네일링 공법이 적용된 굴착 모서리부에 대한 3차원 안정해석 및 거동분석 등에 대한 실험이나 연구결과는 미흡한 실정이며, 따라서 보강재의 배치형태, 삽입각도 및 길이 등 관련 설계변수값 결정에 관하여 주로 경험에 의존하고 있는 실정이다.

따라서 본 연구의 주된 목적은, skew 쏘일네일링 공법이 오목형태 굴착 모서리부에 적용되는 경우 이에 대한 3차원 한계평형 안정성 평가기법을 제시하는 데 있다. 3차원 예상 파괴흙쐐기의 형상은 FLAC^{3D} 프로그램 모델링 및 해석을 통해 결정하였으며, 모서리부에 대한 3차원 침투수압 산정식의 제시 및 해석시 다층지반조건의 고려 등이 포함되었다. 또한 제시된 3차원 안정해석법을 이용해, 관련 설계변수들의 모서리부 안정성에 미치는 영향 정도를 분석하였다. 아울러 기 제시된 볼록형태 굴착 모서리부의 3차원 안정해석법을 이용해 skew 쏘일네일 보강패턴의 효율성을 분석하였으며, 또한 굴착과정을 통해 전면부 벽체변위 및 인접지반의 침하 등이 상대적으로 문제시되는 볼록형태 굴착 모서리부에 대한 변위예측을 위해 준 3차원 유한요소 해석기법 및 중첩기법 등의 적용을 시도하였다.

ABSTRACT

In the present study, a method of the three-dimensional limit equilibrium stability analysis of

*1 Professor, Dept. of Civil Eng., Hong-Ik University
*2 Graduate Student, Dept. of Civil Eng., Hong-Ik university
*3 Engineer, Hyundai Engineering Co., Ltd.
*4 Assistant Professor, Dept. of Civil Eng., Seoil Junior College

the concave-shaped excavation corner reinforced with skew soil nailing system is proposed. A shape of the potential failure wedge for the concave-shaped excavation corner is assumed on the basis of the results of the FLAC^{3D} program analysis. Estimation of the three-dimensional seepage forces expected to act on the failure wedge is made by solving the three-dimensional continuity equation of flow with appropriate boundary conditions. By using the proposed method of three-dimensional stability analysis of the concave-shaped excavation corner, a parametric study is performed to examine the reinforcement effect of skew soil nailing system, range of the efficient skew angles and seepage effect on the overall stability. Also examined is the effect of an existence of the right-angled excavation corner on three-dimensional deflection behaviors of the convex-shaped skew soil nailing walls. The results of analyses of the convex-shaped excavation corner with skew soil nailing system is further included to illustrate the effects of various design parameters for typical patterns of skew nails' reinforcement system

Keywords : Concave-Shaped Corner, Convex-Shaped Corner, Skew Soil Nailing System, 3D Limit Equilibrium Stability Analysis, 3D Seepage Forces, 3D Deflection Behaviors.

1. Introduction

The benefits of utilizing internally reinforced members, such as soil nails and geogrids, in maintaining stable excavations and slopes have been known among geotechnical engineers to be very effective. To date, virtually all-reinforcing members have been installed on a plane perpendicular to the facing wall. However, when the earth reinforcement techniques are to be applied at irregularly shaped areas, such as concave-shaped corner, convex-shaped corner or U-shaped extrusion, it is inevitable to align the reinforcing members at horizontal angles other than 90 degrees to the facing wall in order to maintain the stability and control the anticipated lateral movements by providing sufficient reinforcement to the soil.

Typically, skew angles close to 45 degrees have been used in such instances. To analyze such earth retaining structures with skew reinforcements, truly three-dimensional analysis may have to be used, since the horizontal skew angle and the vertical inclination angle of the reinforcing members are involved. However, to date, no rational but simple-to-use three-dimensional method of analysis of skew earth retaining structures is available.

In the present study, a method of the three-dimensional limit equilibrium stability analysis of the concave-shaped excavation corner reinforced with skew soil nailing system as schematically shown in Fig. 1 is proposed. A shape of the potential failure wedge is assumed on the basis of the results of the FLAC^{3D} program analysis. Seepage forces expected to act on the three-dimensional failure wedge are also taken into account by solving the Laplace's equation with appropriate boundary conditions. By using the proposed method of three-dimensional limit equilibrium stability analysis for a case of the concave-shaped excavation corner, analyses are performed to examine the reinforcement effect of skew soil nailing system, range of the efficient

skew angles and seepage forces' effect on the overall stability.

In addition to the stability analyses of the concave-shaped case, three reinforcement patterns of skew nails are introduced to examine the effect of an existence of the right-angled excavation corner on three-dimensional deflection behaviors of the convex-shaped skew soil nailing walls(refer to the Fig. 1). For each of the three types of skew nails' reinforcement patterns, a tentative relationship is developed for estimating three-dimensional maximum wall deflection and ground surface settlement based on a finite element method of analysis utilizing the generalized plane strain approach. For purposes of further illustration of the skew nails' reinforcement effects, the results of a parametric study based on the method of three-dimensional stability analysis proposed in the previous research paper(Kim et al., 1997) is included in the present study. This parametric study investigates the effectiveness of each of the three types of skew nails' reinforcement pattern, varying the nail spacing, nail installation angle, facing slope angle and nail length.

2. Three-Dimensional Failure Wedge

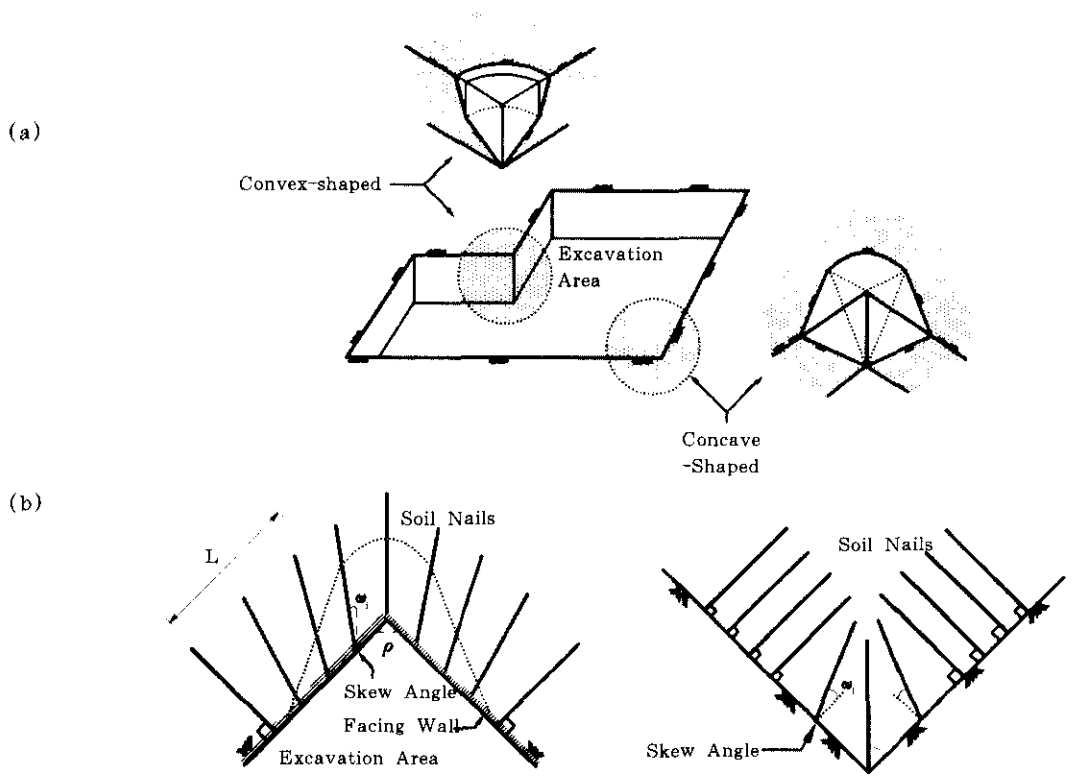

Fig.1 A schematric representation of the irregularly shaped excavation corners with skew soil nailing system

To determine the postulated three-dimensional failure wedge expected in the concave-shaped excavation corner(Fig. 1), FLAC^{3D} program analysis is carried out. In the present study, straight-line excavation zones located at the outer sides of the boundary of skew soil nailing system, which is denoted as L in Fig. 1, are assumed to be fully stable with sufficient reinforcements of soil nailing system. The FLAC^{3D} is a three-dimensional explicit finite difference program widely used for the analyses of soil-structure interaction behaviors.

Pertinent parameters and grid model used in the FLAC^{3D} program analysis are summarized in Table 1 and Fig. 2.

A typical displacement distribution obtained by the FLAC^{3D} program analysis is depicted by the contours in Fig. 3. The postulated three-dimensional failure wedge is approximately estimated by examining the shapes of displacement contours.

Table 1. Pertinent parameters used in the FLAC^{3D} program analysis

Soil Unit Weigth (t/m^3)	Soil Cohesion (t/m^2)	Soil Internal Friction Angle (°)	Nail Length (m)	Nail Installztion Angle(measured from the horizontal axis) (°)	Vertical & Horizontal Spacing of Nail (m)	Total Height of Excavation (m)	Bulk Modulus (t/m^2)	Shear modulus (t/m^2)
1.8	1.0	25	4.25	15	1.0	6.5	5663.2	1887.7

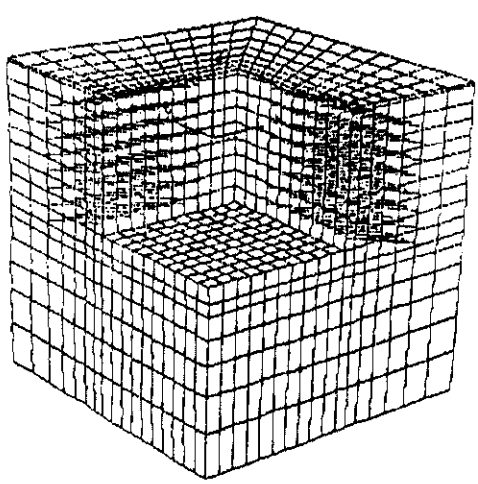

Fig.2 Grid model used in the FLAC^{3D} program analysis

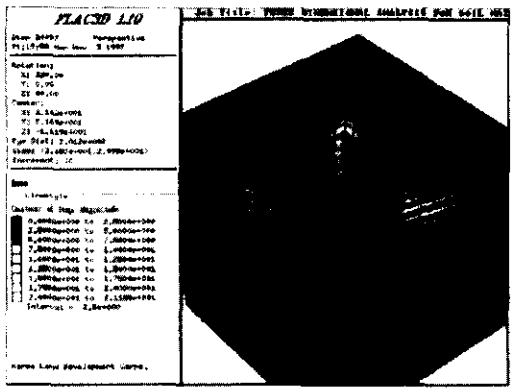

(a) perspective 1

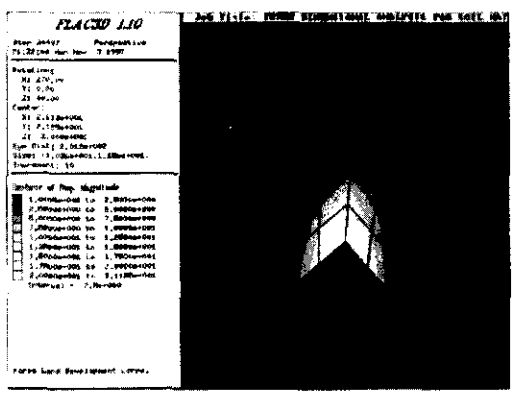

(b) perspective 2

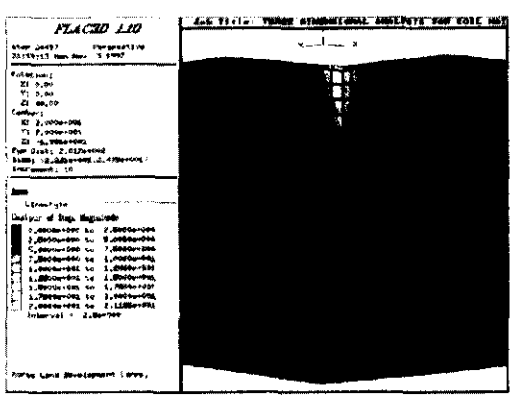

(c) x-y plane

Fig.3 Results of the FLAC^{3D} program analysis (displacement contours)

3. 3D Limit Equilibrium Stability Analysis of the Concave-Shaped Excavation Corner Reinforced with Skew Soil Nails

3.1 Basic Approach

The postulated three-dimensional failure wedge illustrated in Fig. 4 is determined by analyzing the shape of displacement contours described in the previous chapter(refer to Fig. 3). It appears that the postulated three-dimensional failure wedge for a case of the concave-shaped excavation zone reinforced with skew soil nails, may be reasonably assumed to consist of three blocks formed geometrically with a circular arc and straight lines. The concave-shaped corner defined by the angle ρ in Fig. 4 may be composed geometrically of an obtuse angle, a right angle or an acute angle.

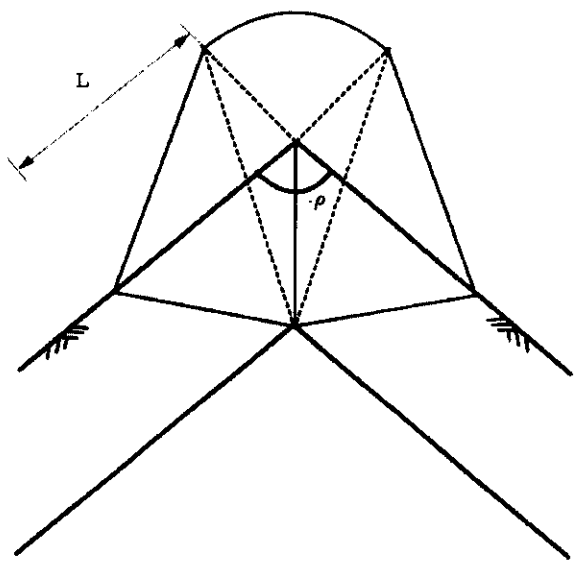

Fig.4 Postulated shape of the three-dimensional failure wedge

Forces acting on each block of the postulated failure wedge may be drawn as shown in Fig. 5. The postulated three-dimensional failure wedge in Fig. 4 is geometrically further defined by the angles α and β. The three-dimensional failure wedge is finalized by iteratively finding a set of angles α and β, which yields the lowest overall factor of safety. The postulated three-dimensional failure wedge is also assumed to extend in both directions to the boundary of skew soil nailing system, which is denoted as L in Figs. 4 and 5.

In Fig. 5, normal forces are expressed as N, and shear forces are expressed as S. Multi-layered soil condition as well as three-dimensional seepage force is also considered in the analysis to deal properly with various field situations actually encountered.

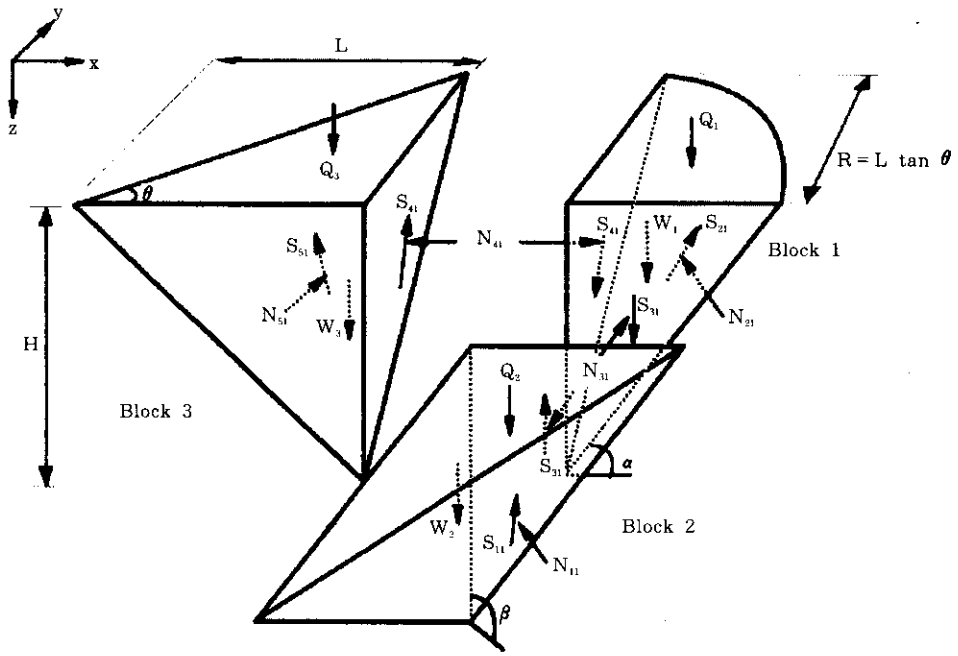

Fig.5 Forces acting on each of the three blocks

3.2 Formulation of Forces Acting on the Block 1

As shown in Fig. 5, the forces acting on the soil block 1 are determined as follows.

$$\overline{W}_1 = \sum_{i=1}^{m} \overline{W_{1i}}, \quad \overline{Q}_1 = q_1 \cdot \frac{\pi \cdot R^2}{4}$$

$$N_{31} = \int_0^R \sum_{i=1}^{m} n_{31i} dx, \quad n_{31i} = \frac{1}{2} K_{ai} \cdot \gamma_i \cdot h_i^2 + h_i \cdot (\sum_{j=1}^{i} K_{aj} \cdot \gamma_j \cdot h_{j-1} \cdot \gamma_{j-1}) \tag{1}$$

$$S_{21} = \overline{\beta} \cdot N_{21}$$

where, $\overline{W}_1$ = weight of the soil block 1, q_1 = surcharge per unit area of ground surface, $\overline{Q}_1$ = total force caused by surcharge q_1, γ_i = soil unit weight of each layer, K_a = coefficient of active earth pressure and $\overline{\beta}$ = ratio between normal and tangential forces.

In Eq. (1), weight $\overline{W}_1$ and acing area of tangential force are estimated by using the Pappus' theorem.

Based on the force equilibrium conditions in x, y and z directions, the corresponding normal and shear forces are determined as follows.

$$N_{21}^{*} = \frac{N_{41} + J \cdot \dfrac{\cos 45^\circ}{\tan \alpha}}{\sin \alpha \cdot \cos 45^\circ + \dfrac{\cos \alpha \cdot \cos 45^\circ}{\tan \alpha}} \tag{2}$$

and,

$$S_{21} = \left[\overline{W}_1 + \overline{Q}_1 - 2 \cdot S_{41} - \left\{ \frac{N_{41} + J \cdot \dfrac{\cos 45^\circ}{\tan \alpha}}{\sin \alpha \cdot \cos 45^\circ + \dfrac{\cos \alpha \cdot \cos 45^\circ}{\tan \alpha}} \cdot \frac{\cos \alpha}{\sin \alpha} \right\} \right] \tag{3}$$

where, $N_{21}^{*} = N_{21} + P_{w21}$, $J = \overline{W}_1 + \overline{Q}_1 - 2 \cdot S_{41}$, and
P_{w21} indicates seepage force possibly caused by the heavy rainfall as well as an existence of the groundwater.

To estimate the ratio $\overline{\beta}$, it is assumed that the driving force expected along the postulated failure surface is equal to the resisting force developed along the same failure surface, i.e.,

$$S_{21} = N_{21} \cdot \tan \phi'_{av} + c'_{av} \cdot Ar_2 \tag{4}$$

where, c'_{av} = developed average soil cohesion, ϕ'_{av} = developed average soil internal friction angle and A represents acting area of developed tangential forces S_{21}. Here, the average soil properties are estimated based on the method proposed by Woods(1990) as follows.

$$c_{av} = \left(\frac{1}{H} \right) \sum_{i=1}^{l+m} c_i h_i, \quad c'_{av} = \frac{c_{av}}{FS_c},$$

$$\text{and} \quad \tan \phi_{av} = \frac{\sum_{i=1}^{l+m} h_i \cdot \gamma_i h_i \cdot \tan \phi_i}{\sum_{i=1}^{l+m} h_i \cdot \gamma_i h_i}, \quad \tan \phi'_{av} = \frac{\tan \phi_{av}}{FS_\phi}$$

where, l+m = total number of soil layers, FS_c = factor of safety with respect to soil cohesion, and FS_ϕ = factor of safety with respect to soil internal friction angle.

Combining with Eqs. (2)~(4) and solving, the ratio between the normal and tangential forces $\overline{\beta}$ is determined as follows.

$$\overline{\beta} = \frac{\left[\overline{W}_1 + \overline{Q}_1 - \left(\dfrac{bb_1}{aa_2} \right) \cdot \cos \alpha \right]}{\left(\sin \alpha - \dfrac{bb_1}{aa_2} - C'_{av} \cdot A\gamma_2^2 \right) \cdot \left(\dfrac{2}{\sin \alpha} - \dfrac{aa_1}{aa_2} \right) \cdot N_{41}} \tag{5}$$

where, $aa_1 = \frac{\cos 45°}{\tan\alpha}\cdot\left(\frac{2}{\tan\alpha} - 2\cdot\tan\phi'_{av}\right)$, $aa_2 = \sin\alpha\cdot\cos 45° + \frac{\cos\alpha\cdot\cos 45°}{\tan\alpha}$, and

$$bb_1 = N_{41} + (\overline{W}_1 + \overline{Q}_1)\cdot\frac{\cos 45°}{\tan\alpha}$$

Since the tangential force cannot be greater than the maximum shear resistance, $N_{41}\cdot\tan\phi'_{av}$, the ratio $\bar{\beta}$ must be smaller than $\tan\phi'_{av}$. Value of the ratio $\bar{\beta}$, therefore, must be positive, i.e.,

$$0.0 \le \bar{\beta} \le \tan\phi'_{av} \tag{6}$$

3.3 Formulation of Forces Acting on the Blocks 2 and 3

As shown in Fig. 5, the forces acting on the soil block 2 are determined as follows.

$$V_1 = \frac{r}{6}\cdot L\cdot\sin\left(\frac{270-\delta}{2}\right)\cdot H,\quad \overline{W}_2 = \gamma'_{av}\cdot V_1$$

$$\overline{Q}_2 = q_2\cdot\frac{R}{2}\cdot L\cdot\sin\left(\frac{270-\delta}{2}\right),\quad N^*_{11} = N_{11} + P_{W11} \tag{7}$$

$$N_{12} = N_{31} - N_{11}\cdot\sin\varepsilon\cdot\tan\theta,\quad N_{13} = \overline{W}_1 + \overline{Q}_1 + S_{31} - N_1\cdot\cos\varepsilon,$$

and, $S_{11} = \sqrt{N_{12}^2 + N_{13}^2}$

where, $\overline{W}_2$ = weight of the soil block 2. $\overline{Q}_2$ = total force caused by surcharge q_2.

The angle β in Fig. 5 between the plane on which the shear force S_{11} acts and the bottom surface is determined as follows.

$$\beta = \cos^{-1}\left(\frac{1}{\sqrt{a^2+b^2+1}}\right) \tag{8}$$

where, $a = \frac{(d_2-d_5)\cdot d_3}{(d_1-d_4)\cdot d_2 - (d_2-d_5)\cdot d_1}$, $b = \frac{(d_1-d_4)\cdot d_3}{(d_1-d_4)\cdot d_2 - (d_2-d_5)\cdot d_1}$

$$d_1 = \frac{H\cdot\cos 45°}{\tan\alpha_1},\quad d_2 = R + \frac{H}{\tan\alpha_1}\cdot\sin 45°,\quad d_3 = H,$$

$$d_4 = -L\cdot\sin\left(\frac{270°-\delta}{2}\right) + \frac{H}{\tan\alpha_1}\cdot\cos 45°,$$

and $$d_4 = -L\cdot\cos\left(\frac{270°-\delta}{2}\right) + \frac{H}{\tan\alpha_1}\cdot\sin 45°$$

Based on the force equilibrium conditions in x, y and z directions, the corresponding normal and shear forces are determined as follows.

$$N_{11} = \frac{\left[\left(\frac{N_{41}\cdot\sin\theta}{\cos\theta}\right)+(\overline{W}_2+\overline{Q}_2+S_{41})\right]}{\sin\varepsilon\cdot\cos\theta+\sin\theta\cdot\tan\theta\cdot\sin\varepsilon+\frac{\cos\varepsilon}{\tan\varepsilon}} \tag{9}$$

and,

$$S_{11} = \sqrt{\left[\frac{N_{41}-N_{11}\cdot\sin\varepsilon\cdot\sin\theta}{\cos\theta}\right]^2+\left[\frac{\overline{W}_2+\overline{Q}_2+S_{41}-N_{11}\cdot\cos\varepsilon}{\sin\varepsilon}\right]^2} \tag{10}$$

The shear force S_{51} acting on the block 3 is equal to S_{11} due to a symmetric condition. The total driving force, S_D, expected along the entire postulated failure surfaces may therefore be expressed as follows

$$S_D = S_{11}+S_{21}+S_{51} \tag{11}$$

The total resisting force, S_F, developed along the entire postulated failure surfaces may also be evaluated as follows,

$$S_F = c'_{av}\cdot(Ar_1+Ar_2+Ar_3)+(N'_{11}+N'_{21}+N'_{51}+\sum T_{TTN})\cdot\tan\phi'_{av}+\sum T_{TTS} \tag{12}$$

where, $T_{TTN} = \sum(T'_n)_i\cdot\cos(90-\eta-\chi)$

$T_{TTS} = \sum(T'_n)_i\cdot\sin(90-\eta-\chi)$

η = slope angle of the wall face

χ = nail inclination angle measured from the horizontal axis

$$Ar_i = \sqrt{s\cdot(s-a)\cdot(s-b)\cdot(s-c)}$$

$$s = \frac{1}{2}(a+b+c)$$

$$p_1 = \frac{h}{\tan\alpha_1}\cdot\cos 45^\circ,\quad p_2 = R+\frac{h}{\tan\alpha_1}\cdot\cos 45^\circ,\quad p_3 = H$$

$$p_4 = -L\cdot\sin\left(\frac{270^\circ-\delta}{2}\right)+\frac{H}{\tan\alpha_1}\cdot\sin 45^\circ$$

$$p_5 = L\cdot\cos\left(\frac{270^\circ-\delta}{2}\right)+\frac{H}{\tan\alpha_1}\cdot\sin 45^\circ$$

$$a = \sqrt{p_1^2+p_2^2+p_3^2},\quad b = \sqrt{p_4^2+p_5^2+p_3^2}$$

$$c = \sqrt{\left[L\cdot\sin\left(\frac{270^\circ-\delta}{2}\right)\right]^2+\left[R-\cos\left(\frac{270^\circ-\delta}{2}\right)\right]^2}$$

$$Ar_2 = \frac{\pi\cdot R}{4}\cdot\frac{H}{\sin\alpha},\quad \text{and}\quad Ar_3 = \frac{1}{2}\cdot R\cdot H$$

3.4 Estimation of Skew Soil Nails' Tensile Forces

The maximum value of skew soil nail tension expressed as T_n in Eq. (12) is expected to occur at the intersection point between the postulated failure surface and the corresponding nail. Value of T_n is estimated by integrating the shear stresses developed between the reinforcing nail and the surrounding soil, based on the mean value over the effective nail length of the normal stresses in the transformed axis which is in the plane perpendicular to the nail, i.e.,

$$T_n = \frac{\pi \cdot d_{hole} \cdot l_n \{(\sigma_n - \sigma_{wr}) \cdot \tan\phi'_{av} + c'_{av}\}}{S_h} \leq \frac{A_{ref} \cdot f_y}{S_h} \tag{13}$$

where, d_{hole} = drilled-hole diameter of reinforcing element, l_n = effective length of n^{th} nail, σ_n = mean value of the normal stresses, σ_{wr} = seepage pressure acting on the nail, A_{ref} = cross-sectional area of the reinforcing element and f_y = tensile yield strength of the nail.

3.5 Evaluation of Overall Stability

Based on the equilibrium conditions, the three-dimensional overall stability of the concave-shaped excavation zone reinforced with skew soil nails may be evaluated. At any stage of analysis, the total driving force and the total developed resisting force along the postulated three-dimensional failure wedge surfaces must be equilibrium state, i.e.,

$$S_D = S_F \tag{14}$$

The overall factor of safety of the concave-shaped excavation zone with skew nails' reinforcement system, FS, is estimated on the basis of the Taylor's criterion, i.e.,

$$FS_C = FS_\phi = FS \tag{15}$$

The factor of safety with respect to average cohesion and friction is regarded as the ratio between the available average cohesion and friction and the developed average cohesion and friction, i.e.,

$$c'_{av} = c_{av} / FS, \quad \tan\phi'_{av} = \tan\phi_{av} / FS$$

By solving the derived equilibrium equations, the overall three-dimensional factor of safety of the concave-shaped excavation zone with skew nails' reinforcement system, FS, can be determined. An iterative solution procedure for determination of FS is necessary for various angles, α and β in Fig. 4, defining shapes of the postulated failure wedge.

4. 3D Seepage Forces Acting on the Postulated three-Dimensional Failure Wedge

The heavy rainfall as well as an existence of the groundwater may cause in-situ soils to be saturated, resulting in an unstable state of the nailed-soil wall due to a decrease of soil shear strengths and a significant increase of the pore water pressures. Expanding the Laplace's

equation, Gray (1958) proposed an analytical solution method of 2D seepage flow. To deal appropriately with the stability of the concave-shaped skew nail reinforcement system, equations necessary to analyze the three-dimensional seepage pressures are derived based on the Gray's approach. Three-dimensional continuity equation of a seepage water is described below and flow conditions considered in the analysis is illustrated in Fig. 6.

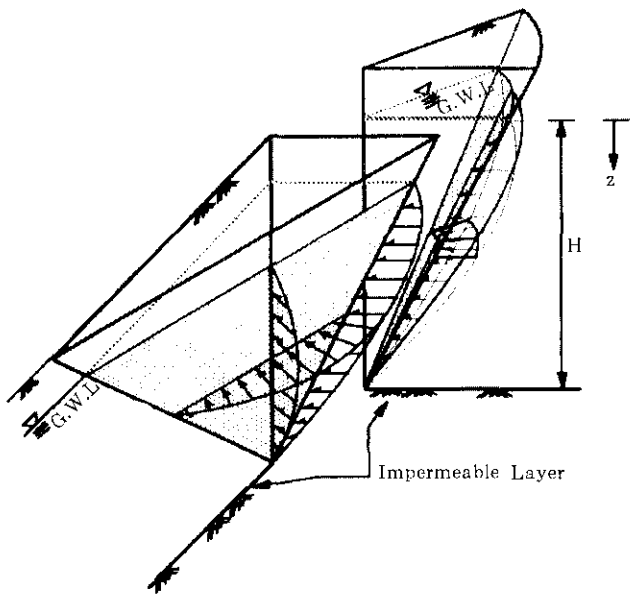

Fig.6 A schematic representation of the three-dimensional seepage flow in the concave-shaped excavation corner

$$\frac{\partial^2 h}{\partial r^2}+\frac{1}{r}\cdot\frac{\partial^2 h}{\partial \theta^2}+\frac{1}{r^2}\cdot\frac{\partial^2 h}{\partial \theta^2}+\frac{\partial^2 h}{\partial z^2}=0 \tag{16}$$

The general solution of Eq. (16) is expressed as follows.

$$h(x,\ y,\ z)=H-R(r)\cdot\Theta(\theta)\cdot Z(z) \tag{17}$$

where, $R(r)=a_1\cdot r^{k_1}+a_2\cdot r^{-k_1}$, $Z(z)=a_3\cdot\cos\frac{k_2}{r}\cdot z+a_4\cdot\sin\frac{k_2}{r}\cdot z$ and

$$\Theta(\theta)=a_5\cdot\cos k\theta+a_6\cdot\sin k\theta$$

Necessary boundary conditions to solve the Eq. (17) are described below.

$$h(\infty,\ \theta,\ z)=H,\quad h(r,\ \theta,\ 0)=H$$

$$\left.\frac{\partial h}{\partial z}\right|_{z=H}=0,\ h(r,\ \theta,\ 0)=H-z,\ \text{and}\ h\left(r,\ \frac{4}{3}\pi,\ z\right)=H-z$$

Solving the Eq. (17) with the above boundary conditions, the particular solution is then obtained as follows.

$$h(x,\ y,\ z) = H - \sum_{m=0}^{\infty} \frac{2}{H} \frac{\sin M - \frac{M}{H} \cdot \pi \cdot r \cdot \cos M}{\left(\frac{M}{H}\right)^2} \cdot \sin\left(\frac{M}{H}\right) \cdot z(\cos k\theta + \sin\theta) \tag{18}$$

where, $M = \frac{(2m+1) \cdot \pi}{2}$

Neglecting the velocity head, the hydraulic head h at any point along the postulated failure surfaces is simply determined by summing the fluid pressure head h_p and the elevation head h_e. Note that the fluid pressure h_p at any point is expressed as

$$h_p = h - h_e = h - (H - z) \tag{19}$$

Seepage pressure σ_w can then be estimated as follows.

$$\sigma_w = \gamma_w \cdot (h - H + z) = \gamma_w \left\{ z + \sum_{m=0}^{\infty} \frac{2}{H} \frac{\sin M - \frac{M}{H} \cdot r \cdot \cos M}{\left(\frac{M}{H}\right)^2} \cdot \sin\left(\frac{M}{H}\right) \cdot z(\cos k\theta + \sin\theta) \right\} \tag{20}$$

The sum of seepage pressures acting on the postulated failure surfaces is calculated by using the 4-point Gauss quadrature numerical technique.

5. Analyses 1(Concave-Shaped Case)

By using the proposed method of three-dimensional limit equilibrium stability analysis of the concave-shaped excavation corner, basic analyses are performed to examine the reinforcement effect of the skew soil nailing system, range of the efficient skew angles and seepage effect on the overall stability. Properties of multi-layered soils and reinforcements used in the analyses are described in Tables 2 and 3, respectively. A schematic sectional representation of the skew nailed-wall analyzed is given in Fig. 7.

Table 2. Properties of the multi-layered soils used in the analyses

Soil Layers	Depth (m)	Soil Cohesion (t/m^2)	Soil Internal Friction Angle (°)	Soil Unit Weight (t/m^3)
Layer #1	0~3m	0.5	25	1.75
Layer #2	3~10m	1.0	30	1.80
Layer #3	Below 10m Depth	1.5	35	2.10
Total Excavation Height	16m			

Table 3. Properties of the reinforcements used in the analyses

Reinforcements	Drilled-Hole Diameter (mm)	Nail Diameter (mm)	Nail Length (m)	Tensile yield Strength of Nail (kg/cm^2)
Nail & Cement Grouting	100	25	12	3600

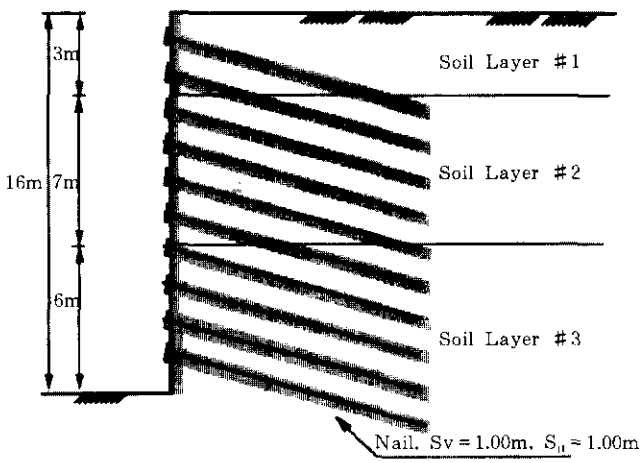

Fig.7 Schematic sectional representation of the skew nailed-wall system analyzed

For a case of the unreinforced excavation corner with properties of multi-layered soils described in Table 2, a relationship between the factor of safety FS and the angle α (refer to Fig. 5) defining the failure wedge is analyzed, and the result is shown in Fig. 8. From the result of Fig. 8, the minimum safety factor FS_{min} is estimated as 0.952, and the corresponding angle α against this state of stability yields approximately as 68°. In this analysis the angle ρ (refer to the Figs. 4 and 5) geometrically defining the concave-shaped excavation corner is assumed to be 90°.

Skew nails' reinforcement system described in both Table 2 and Fig. 7 is therefore applied to improve the stability. The effect of skew nails' reinforcement system is investigated, varying the skew angle ω_i. Note that the surcharge load is not considered in this analysis, and the groundwater in seepage case is assumed to exist at the top ground surface. It is further noted that the skew angle ω_i of each nail denoted in the previous Fig. 1 is assumed to be uniform in this analysis.

Analyzing the results illustrated in Figs. 9 and 10, it is realized that the efficient skew angle ω of the nails (refer to Fig. 1) lies approximately in the range of 17~18°. It is also analyzed from the Figs. 9 and 10 that the factors of safety FS decrease by about 10.3% due to seepage effects.

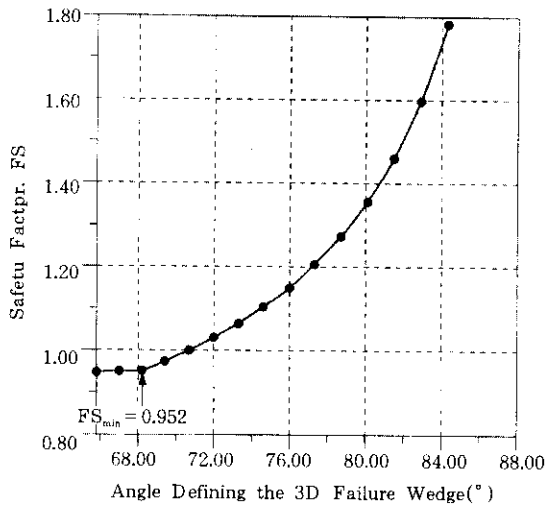

Fig.8 Relationship between the safety factor FS and the corresponding angle α defining the unreinforced soil wedge

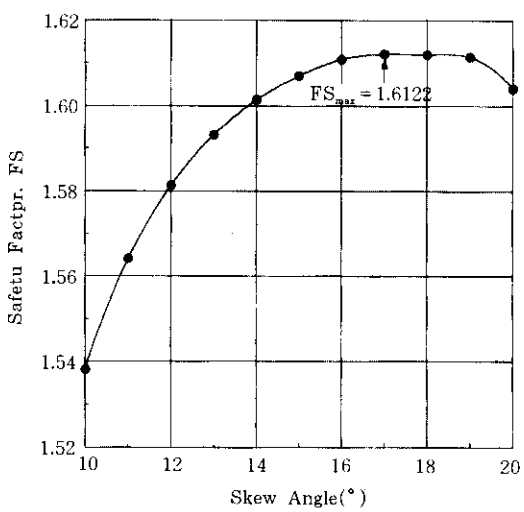

Fig.9 Relationship between the safety factor FS and the corresponding skew angle ω of the nails

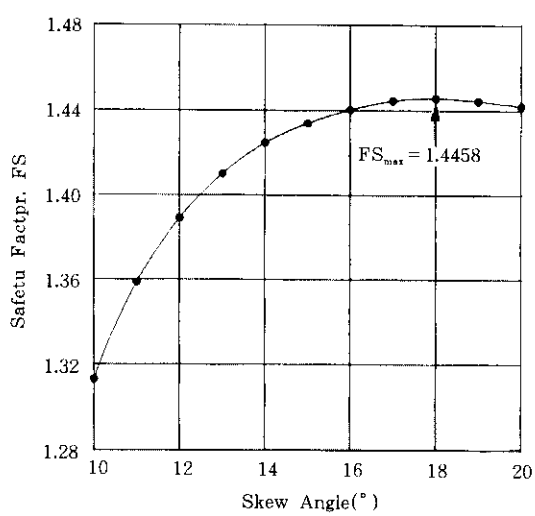

Fig.10 Relationship between the safety factor FS and the corresponding skew angle ω of the nails(seepage case)

6. Analyses 2(Convex-Shaped Case)

6.1 Analysis of reinforcement pattern

Based on the same soil properties described in Table 2 and by using the procedure described in the previous research paper(Kim et al., 1997), overall stability analysis is further made for a case of the convex-shaped unreinforced excavation corner shown in Fig. 1. A case of the right-angled excavation corner is dealt with in this analysis. The minimum safety factor FS_{min} is evaluated as 0.727(Kim et al., 1997), and skew nails' reinforcement system described in both Table 3 and Fig. 8 is also applied to improve the stability.

The effectiveness of each of the three types of skew nails' reinforcement pattern indicated as *Case 1*, *Case 2* and *Case 3* in Fig. 11 is analyzed, varying the nail vertical spacing S_v , nail installation angle α, facing slope angle η and nail length L_n. Skew angles ω_i of the nails adopted for each type of the reinforcement pattern are described in Fig. 11. Note that seepage force and surcharge load are not considered in this analysis.

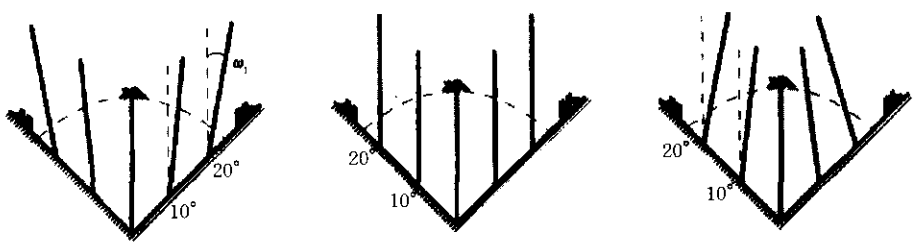

(a) Case 1 (b) Case 2 (c) Case 3

Fig.11 Skew nails' reinforcement patterns

Analyzing the results illustrated in Figs. 12~15, it may be concluded that *Case 1* is most effective among the three types of reinforcement pattern, and *Case 2* is a relatively efficient reinforcement pattern compared to the *Case 3*. In view of the stability, the range of efficient nail installation angle α is between $8^\circ \sim 15^\circ$ regardless of the types of reinforcement pattern. The differences in factors of safety for various nail vertical spacing, nail installation angles, facing slope angles and nail lengths are relatively small between *Case 1 and 2*. *Case 3* yields, however, the lowest factors of safety compared to both *Cases 1 and 2*.

6.2 Analysis of three-dimensional deflection behaviors

Except overall stability analysis of the skew nailing reinforcement system previously analyzed, prediction of excavation wall deflection and ground surface settlement is a very important issue especially when the skew nailing reinforcement system is applied at the convex-shaped excavation areas. To properly analyze such deflection behaviors of the skew soil nailing walls,

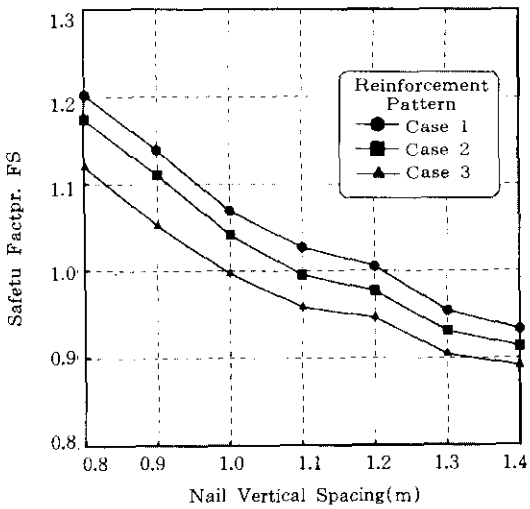

Fig.12 Effect of nail vertical spacing S_v

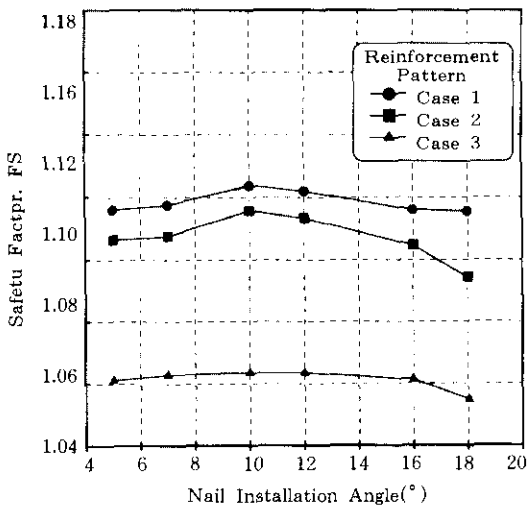

Fig.13 Effect of nail installation angle α

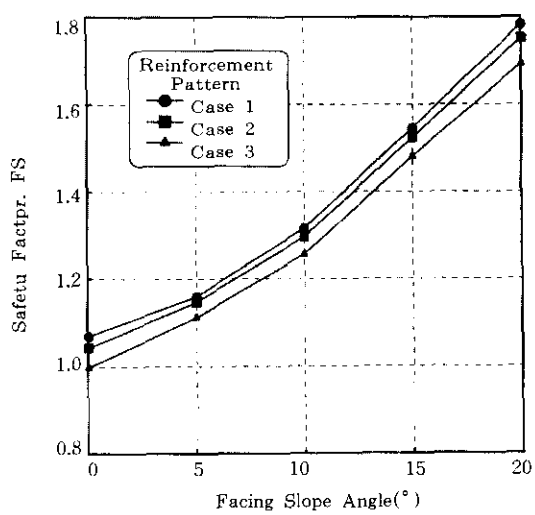

Fig.14 Effect of facing slope angle η

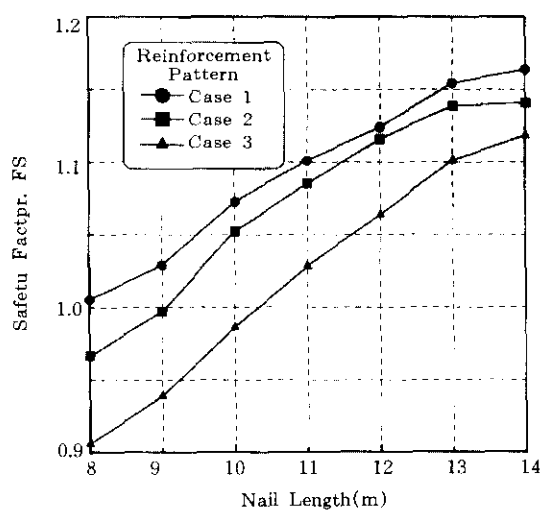

Fig.15 Effect of nail length L_n

truly three-dimensional analysis may have to be used. However, a three-dimensional analysis of deep excavation is generally considered difficult to approach due to the large computer storage and enormous computation time required. As an alternative, an approximate relationship is secured in the present study for estimating three-dimensional maximum wall deflection and ground surface settlement based on a finite element method of analysis utilizing the generalized plane strain approach(Bang, S., 1988).

The generalized plane-strain approach simply assumes that the plane strain directional strain, ε_z, remains zero instead of the plane-strain directional displacement, w, being zero, as is commonly adopted in the conventional plane strain approach. Therefore, the approach includes three non-zero displacement components u, v and w along the x, y and z coordinates, none if it is dependent on the out-of-plane coordinate, z. The main advantage of this approach is that it may be able to calculate the three-dimensional stresses and displacements while the coordinate system remains in two dimensions, thus making it ideally suited for the finite element analysis. However, it is noted that direct application of this approach is limited to the case having a constant angle between the principal axis of the material orthotropy and the out-of-plane coordinate.

Therefore, further adopting the concept of superposition applied to the displacement analysis of a root pile system(Kim et al., 1997), the following expression is formulated in the present study to predict maximum wall deflection and ground surface settlement of the convex-shaped excavation corner reinforced with soil nailing system.

$$\delta = \mathrm{GPSR} \cdot \frac{\sum_{i=1}^{n} \mathrm{DR}_i}{n} \cdot \sum_{i=1}^{n} (\delta_{set})_i \tag{21}$$

where, DR defined as $\frac{\delta_{sh}}{\delta_{set}} \leq 1.0$ represents a ratio of displacements estimated based on two different horizontal spacing of skew nails. A scheme of this approach is illustrated in Fig. 16 and the detailed concept is given in the reference paper(Kim, et al., 1997).

Also, generalized plane strain ratio denoted as GPSR in the above Eq. (21) describes an approximate relationship between the results of three-dimensional maximum wall deflection and ground surface settlement evaluated by the FLAC^{3D} program analysis and those predicted on the basis of the generalized plane strain(GPS) analysis. The expression of Eq. (21) may be regarded as a tentative relationship. It is believed that the many more factors affecting excavation deflection behaviors can be incorporated to obtain a more general relationship.

For each of the three types of reinforcement patterns, GPS analysis is independently performed for different skew angles, and the result is superposed on the basis of the method as schematically illustrated in Fig. 16 and by using the Eq. (21).

A schematic configuration of the right-angled excavation section analyzed is shown in Fig. 17, and relevant material properties with geometric condition are summarized in Table 4. Seepage effect is not considered in this analysis.

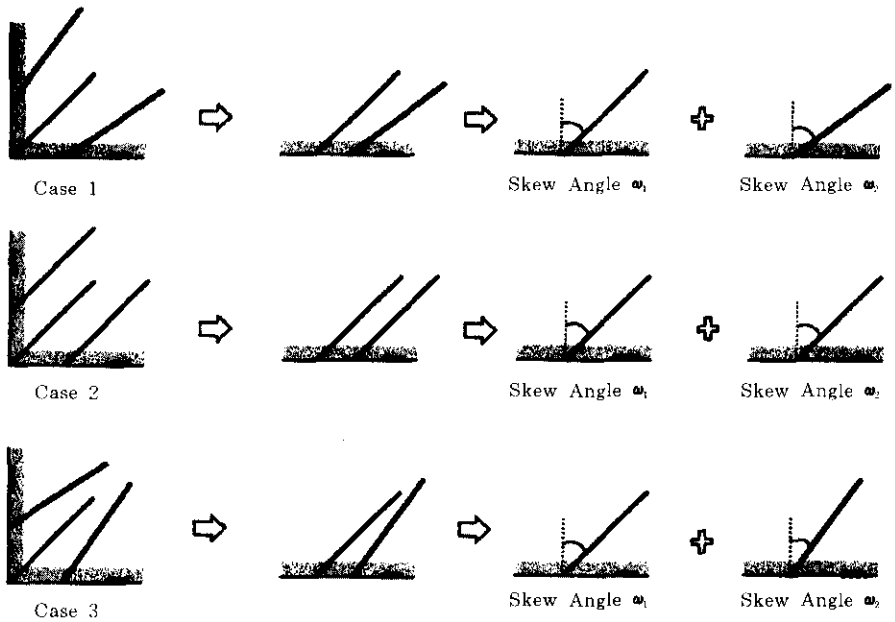

Fig.16 A Scheme of the superposition technique applied to the analysis of deflection behaviors

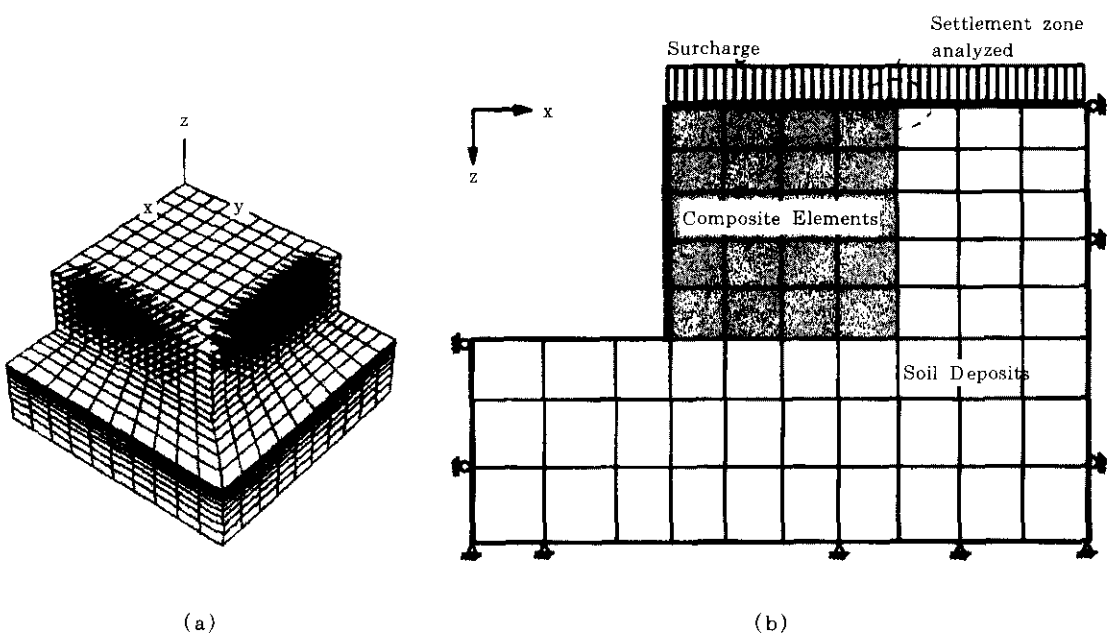

Fig.17 Meshes used in the analyses of the FLAC^{3D} program and GPS

Table 4. Relevant material properties used in the analyses of the FLAC^{3D} program and GPS

Geometric Condition	Total Excavation Depth = 6m, Wall Inclination Angle = 90° (Wall facing is assumed to be vertical)
Soil Properties	Elastic Modulus = 50000kPa, Poisson's ratio = 0.35
Properties of Reinforcements	Drilled Hole Diameter = 10cm, Nail Length = 4m, Nail Diameter = 25mm Vertical & Horizontal Installation Spacing of Nail : S_V = 1.0m , S_H = 2.0m
Applied Surcharge Loads	Up to 40 t/m^2

For each of the three types of reinforcement patterns indicated as Case 1, Case 2 and Case 3 in Fig. 16, approximate relationships defined as GPSR in Eq. (21) are investigated based on the comparisons between the results of maximum wall deflections and ground surface settlements evaluated by the FLAC^{3D} program analyses and those predicted by the GPS analyses. Analyzing the comparisons of maximum wall deflections as summarized in Table 5, it is found that the range of GPSR defined in Eq.(21) is about 1.69~2.11. It is also found that the range of GPSR for a case of ground surface settlement is about 1.58~1.75. Typical results for the Case 1 are illustrated in Figs. 18 and 19. Similar to the previous findings concerned with the reinforcement effect on overall stability, it is concluded that Case 1 results in the least wall deflection and ground surface settlement are compared to the other types of reinforcement patterns.

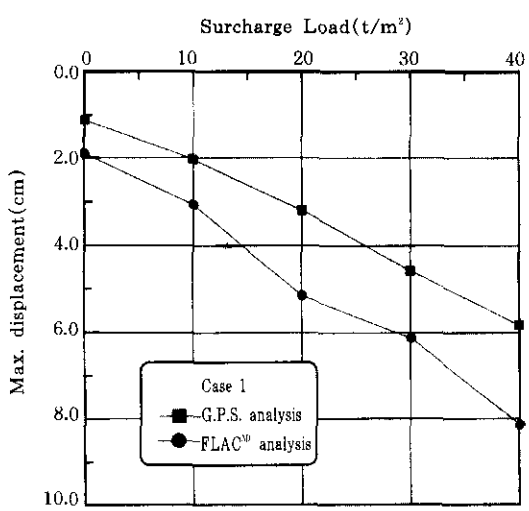

Fig.18 Comparison of the maximum wall deflection.Case1

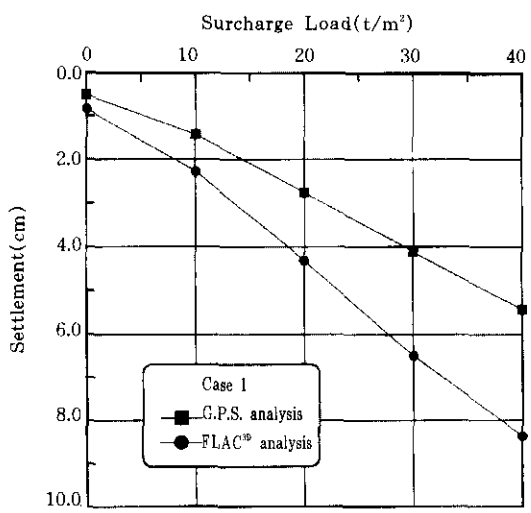

Fig.19 Comparison of the ground surface settlement/Case1

Table 5. Approximate relationships between the results of FLAC^{3D} program analyses and GPS analyses

	Values of GPSR in Eq.(21)	
	Maxium wall deflection	Ground surface settlement
Case 1	1.69	1.58
Case 2	1.87	1.66
Case 3	2.11	1.75

6. Conclusions

In the present study, a method of the three-dimensional limit equilibrium stability analysis of the concave-shaped excavation corner reinforced with skew soil nailing system is proposed. A shape of the potential failure wedge is assumed on the basis of results of the FLAC^{3D} program analysis. Seepage forces expected to act on the three-dimensional failure wedge are also taken into account by solving the Laplace's equation with appropriate boundary conditions. By using the proposed method of three-dimensional limit equilibrium stability analysis for a case of the concave-shaped excavation corner, analyses are performed to examine the reinforcement effect of skew soil nailing system, range of the efficient skew angles and seepage forces' effect on the overall stability.

In addition to the stability analyses of the concave-shaped case, three reinforcement patterns of skew nails are introduced to examine the effect of an existence of the right-angled excavation corner on three-dimensional deflection behaviors of the convex-shaped skew soil nailing walls. For each of the three types of skew nails' reinforcement patterns, a tentative relationship is developed for estimating three-dimensional maximum wall deflection and ground surface settlement based on a finite element method of analysis utilizing the generalized plane strain approach. For purposes of further illustration of the skew nails' reinforcement effects, the results of a parametric study based on the method of three-dimensional stability analysis proposed in the previous research paper(Kim et al., 1997) is included in the present study. This parametric study investigates the effectiveness of each of the three types of skew nails' reinforcement pattern, varying the relevant design parameters.

Systematic experimental studies may be necessary to verify the proposed three-dimensional analytical method of stability analysis for the irregularly shaped excavation corner reinforced with skew soil nailing system.

References

1. Bang, S.(1988), *Design and Analysis of Reinforcing Distressed Bridge Abutments*, Final Report to South Dakota Department of Transportation.
2. Baligh, M.M. and Azzouz, A.S.(1975), "End Effects on Stability of Cohesive Slopes", *ASCE, Journal of*

Geotechnical Engineering, Vol. 101, No. GT11, pp. 1105~1117.

3. Chen, R.H. and Chameau, J.L.(1982), "Three-Dimensional Limit Equilibrium Analysis of Slopes", *Geotechnique*, Vol. 32, No. 1, pp.31~40.
4. Leshchinsky, D. and Baker, R.(1986), "Three-Dimensional Slope Stability : End Effects", *Soils and Foundations*, Vol. 26, No. 4, pp.98~110.
5. Duncan, J. M. and Chang, C. Y.(1970), "Nonlinear Analysis of Stress and Strain in Soils", *ASCE. Journal of the Soil Mechanics and Foundations Division*, Vol. 96, No. SM5, pp.1629~1653.
6. Gabriel, F. and Tirso, A. A. Jr.(1994), "Seepage-Induced Effective Stresses and Water Pressures Around Pressure Tunnels", *ASCE, Journal of Geotechnical Engineering*, Vol. 120, No. 1, pp.108~128.
7. Gassler, G.(1988), "Soil Nailing Theoretical Basis and Practical Design", Proceeding of the Geotechnical Symposium on Theory and Practice of Earth Reinforcement, Balkema, pp.283~288.
8. Gray, H.(1958), "Contribution to the Analysis of Seepage Effects in Backfills", *Geotechnique*, Vol. 8, No. 4, pp.166~170.
9. Kim, H.T. , Kang, I.K. and Park, S.W.(1997), "Method of Quasi-Three Dimensional Stability Analysis of the Root Pile System on Slope Reinforcement", Proceedings of the KGS spring '97 National Conference, pp. 101~123
10. Kim, H.T., Lee, E.S., Hwang, Y.C. and Park J.Y.(1997), "Three-Dimensional Limit Equilibrium Stability Analysis of L-shaped Corner with Skew Soil Nailing System", Proceeding of the 30th Year Aniversary Symposium of SEAGS, Bangkok, Thailand, pp. 5-62~5-75.
11. Woods, R.I. and Jewell, R.A.(1990), "A Computer Design Method for Reinforced Soil Structures", *Geotextile and Geomembranes 9*, pp. 233~259.

(received on May, 4, 1998)